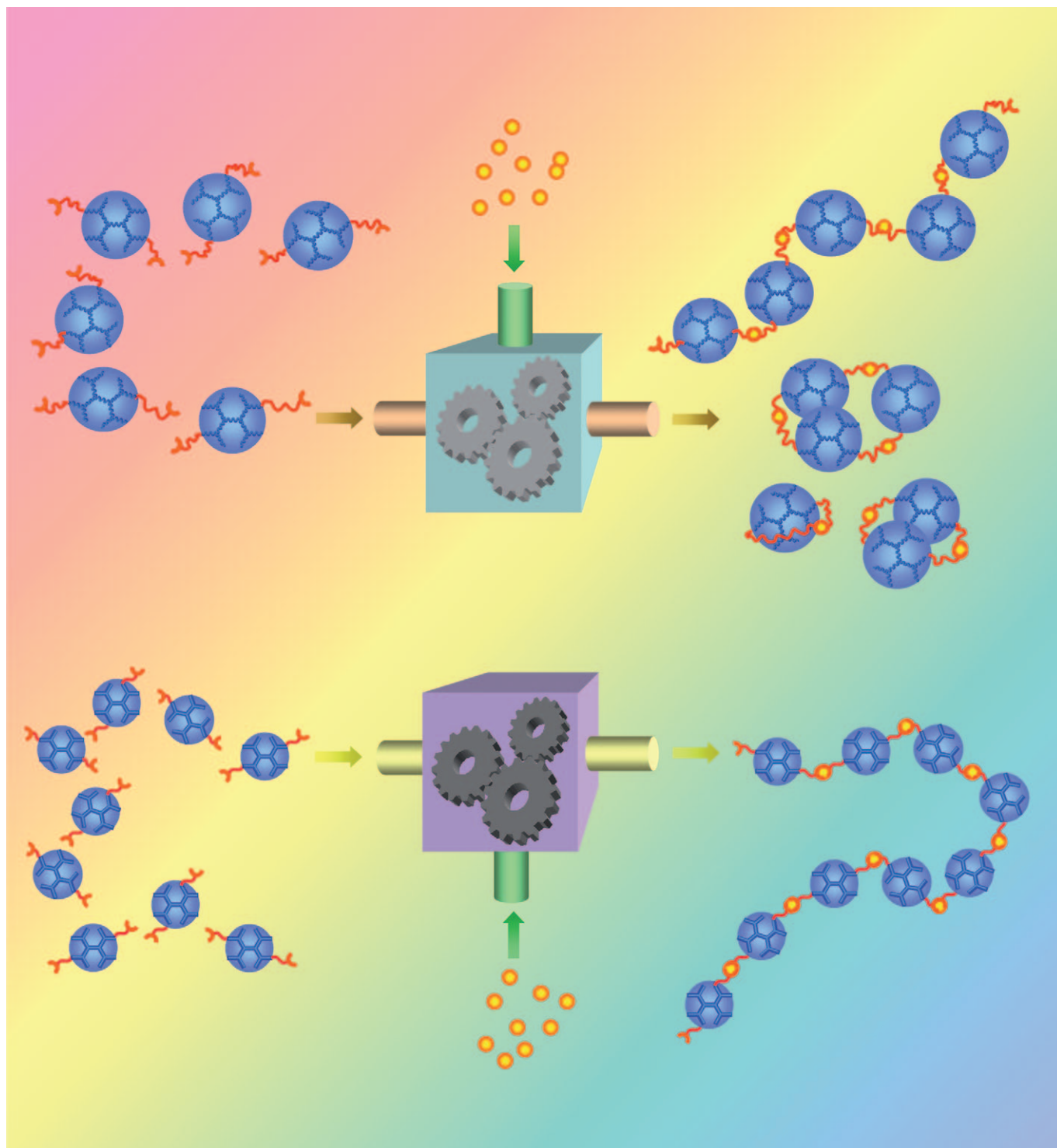


Synthesis of Organometallic Poly(dendrimer)s by Macromonomer Polymerization: Effect of Dendrimer Size and Structural Rigidity on the Polymerization Efficiency

Siu-Yin Cheung,^[a] Hak-Fun Chow,*^[a, b] To Ngai,^[a] and Xiaoling Wei^[a]



Abstract: Two series of first to third generation (G1–G3) oligoether dendrimers, one bearing a shorter spacer chain (C–O) and the other having a longer spacer branch (C–C–C–O) were prepared. Both series of compounds, containing two reactive C≡CH moieties on the dendrimer surface, were used as macromonomers and copolymerized with *trans*-[Pt(PEt₃)₂Cl₂] to form organometallic poly(dendrimer)s by an outer-sphere–outer-sphere connection strategy. It was found that

concentration of monomer used in the polymerization, the dendrimer generation, and, most strikingly, the length of the spacer were key factors that determined the polymerization efficiency. Hence, the structurally more rigid and compact C–O linked dendrimers formed poly(dendrimer)s with a higher degree of polymerization than the

structurally less rigid and more bulky C–C–C–O dendrimers. This result was due to the higher tendency to form cyclic oligomers in the latter series of compounds. In addition, the differences in the polymerization efficiency among the three generations of dendrimers could be explained by the gradual decrease of reactive functional group density on the dendrimer surface.

Keywords: dendrimers • platinum • polymerization • polymers

Introduction

The use of dendrons or dendrimers as building blocks for the synthesis of more complex polymer architectures is a topic of current interest. Several classes of novel structures, namely dendrimer–linear polymer hybrids,^[1] dendronized polymers,^[2] and poly(dendrimer)s,^[3] have appeared (Figure 1). Although there are numerous examples based on

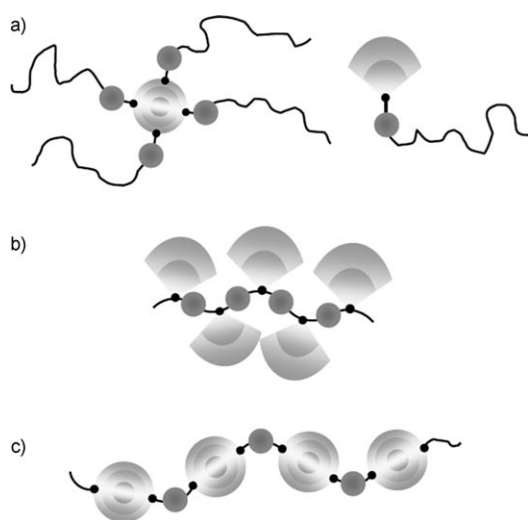


Figure 1. Schematic drawings of a) dendrimer–linear polymer hybrids, b) a dendronized polymer, and c) a poly(dendrimer).

the first two classes of compounds, reports on the synthesis and properties of poly(dendrimer)s are rare. Dendrimer–linear polymer hybrids can be conveniently accessed synthetically by attaching multiple linear polymer chains to the surface functionalities or one linear polymer chain to the focal point of a dendron. In contrast, dendronized polymers may be prepared through the graft-to, graft-from, or macromonomer polymerization strategies.^[2] Invariably, all three methods involve reactions at the focal point functional group (i.e. inner-sphere–inner-sphere connection)^[4] of a dendron. As a result, steric inhibition could become a major synthetic problem, especially in the formation of dendronized polymers bearing higher generation dendritic side chains. Some time ago we reported the direct 1:1 copolymerization of *trans*-[Pt(PEt₃)₂Cl₂] and dendrimers **1** bearing two reactive functional groups on the surface of an oligoether dendrimer to form poly(dendrimer)s **2**^[5] and anticipated that steric hindrance could be alleviated by using an outer-sphere–outer-sphere connection strategy.^[4] Because of their structural resemblance to necklaces, they were also called dendritic necklaces. In this particular study, we deliberately installed the reactive C≡CH functionality at the end of an elongated C-10 surface functionality with the aim to improve the polymerization efficiencies. As it turned out, the degree of polymerization (DP) value was 10³ (based on laser light scattering data) for first generation (G1), 10² for second generation (G2), and 30 for third generation (G3) bifunctional dendrimers (Figure 2).

[a] S.-Y. Cheung, Prof. Dr. H.-F. Chow, Prof. Dr. T. Ngai, X. Wei
Department of Chemistry, The Chinese University of Hong Kong
Shatin, NT, Hong Kong SAR (China)
Fax: (+852)2603-5057
E-mail: hfchow@cuhk.edu.hk

[b] Prof. Dr. H.-F. Chow
The Center of Novel Functional Molecules
The Chinese University of Hong Kong (China)

Supporting information for this article is available on the WWW under <http://dx.doi.org/10.1002/chem.200802306>.

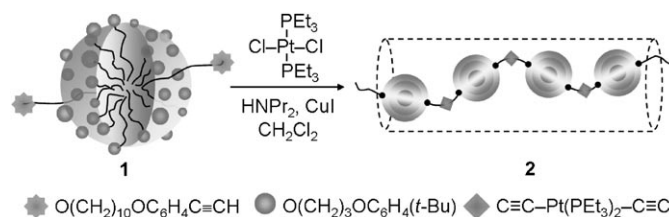
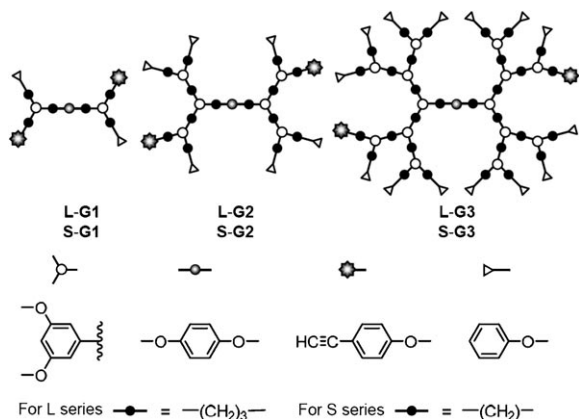


Figure 2. Synthesis of poly(dendrimer)s **2** from surface bifunctional macromonomers **1**.

To better evaluate this new approach for the synthesis of poly(dendrimer)s, it is necessary to carry out a thorough investigation of how the various structural factors can affect the polymerization efficiency. Herein, we report 1) the controlled syntheses of two different series of G1–G3 surface-bifunctional oligoether dendrimers, one containing a shorter C–O branch skeleton **S-Gn** ($n=1-3$), and the other **L-Gn**



($n=1-3$) containing a longer C–C–C–O branch, in high yields and excellent purity, 2) their 1:1 copolymerizations with the linker *trans*-[Pt(PEt₃)₂Cl₂] through the surface C≡CH units, and 3) the dependence of the polymerization efficiency on the structural flexibility and molecular size of the dendritic macromonomers. A comparison of the polymerization results of these two series of dendrimers, which differ only by the length of the branches, is made to resolve the issue of whether the structural rigidity of the branches may have an effect on polymerization. It was also of interest to see whether the polymerization of such large macromonomers with two reactive groups located at distant locations has any different characteristics from those of conventional small monomer molecules.

Results and Discussion

Retrosynthetic analysis: The specific installment of only two reactive surface groups on a dendrimer surface containing multiple surface functionalities is by no means an easy task. There are many complicating factors that one should consider before carrying out the synthesis. First, only two, not one or three, reactive groups should be decorated on the surface. Second, the purity of the bifunctional dendrimers should be extremely high. If, as a result of some synthetic flaws, 1% of a monofunctional dendrimer is formed as a by-product mixed with 99% of the bifunctional dendrimer, this monofunctional dendrimer will then serve as a polymer chain stopper, and the theoretical maximum DP value will become 200. Similarly, if the macromonomer sample contains 1% of a trifunctional macromonomer, a network structure will be formed after polymerization. Third, the pres-

ence of 1% of monofunctional or trifunctional impurities is not easily detectable by ¹H NMR spectroscopy or size-exclusion chromatography (SEC) because of their structural and size resemblance, and hence one cannot rely only on spectroscopic means to confirm their purity. Rather, it is absolutely necessary to design a synthetic route that can guarantee the formation of the target bifunctional macromonomers in extremely pure form.

The retrosynthetic analysis of the bifunctional macromonomers **L-Gn** and **S-Gn** is shown in Figure 3. Apart from

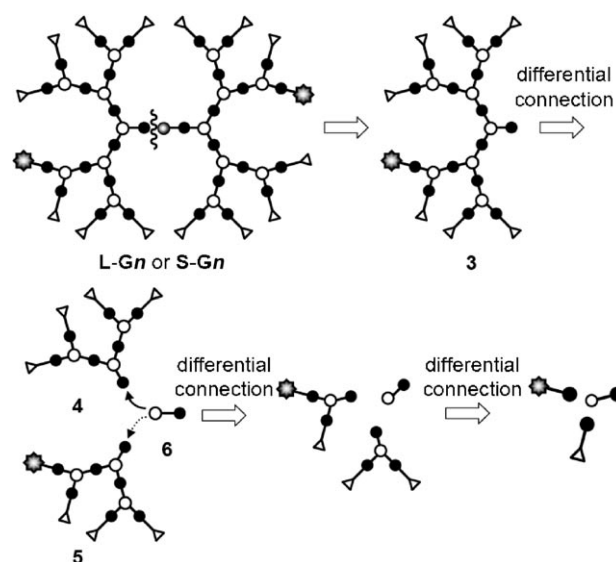
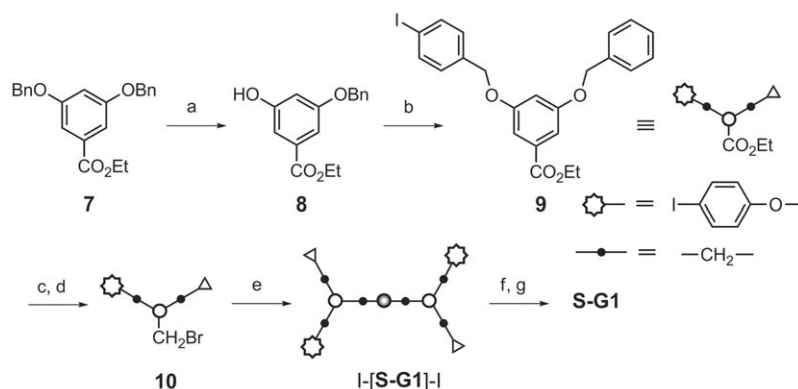


Figure 3. Retrosynthetic analysis of surface bifunctional macromonomers **L-Gn** and **S-Gn**.

the final coupling step of a dendron **3** to the central core to produce the target compounds, all other operations involve the differential connection of a branching unit **6** to two different dendrons, that is, one symmetrical dendron (e.g. **4**) and one unsymmetrical dendron (e.g. **5**). To avoid installment of two identical dendrons to the branching unit **6**, one must exert complete control on the selective coupling of the branching unit **6** to two different dendrons. This can be accomplished either by controlling the reactant stoichiometry of the coupling reaction or by creating an appropriately protected branching unit. In addition, as the terminal acetylene functionality is relatively labile, we plan to install it by Sonogashira coupling^[6] to the corresponding aryl iodide at the postdendrimerization stage. Hence, our initial objective was to prepare the two different series of surface diiodo-functionalized dendrimers I-[**S-Gn**]-I and I-[**L-Gn**]-I.

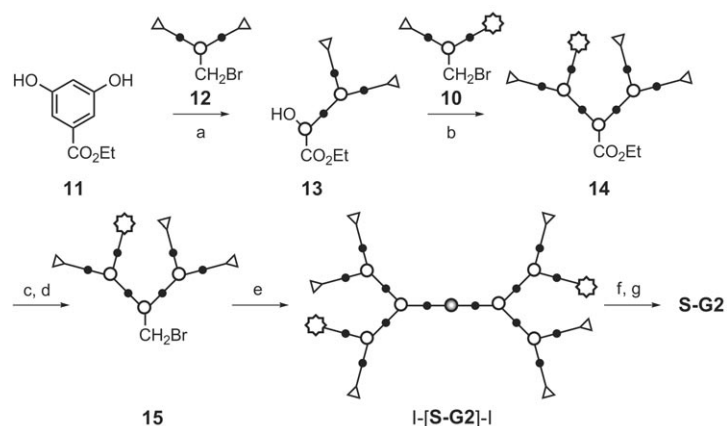
Synthesis of S-Gn dendrimers: The starting material for the short (C–O) branching unit was ethyl 3,5-dibenzyloxybenzoate **7** (Scheme 1). Controlled partial hydrogenolysis of compound **7** in the presence of 10% Pd on C in EtOAc/EtOH (1:1) at 20 °C afforded the monobenzylated branching unit **8** in 52% yield. The fully deprotected ethyl 3,5-dihydroxybenzoate and the unreacted starting material **7** could



Scheme 1. Synthesis of **S-G1**. Reagents and conditions: a) H_2 , 10% Pd/C, EtOAc/EtOH 1:1, 25 °C, 2 h, 52%; b) 4-iodobenzyl bromide, K_2CO_3 , [18]crown-6, acetone, 56 °C, 12 h, 97%; c) DIBAL-H, hexane, $-60\text{ }^\circ\text{C}$ – $0\text{ }^\circ\text{C}$, 2 h, 52%; d) PPh_3 , CBr_4 , THF, 25 °C, 2 h, 61%; e) hydroquinone (0.45 equiv), Cs_2CO_3 , dibenzo-[24]crown-8, DMF, 25 °C, 12 h, 85%; f) $\text{TMSC}\equiv\text{CH}$, CuI, $[\text{Pd}(\text{PPh}_3)_2\text{Cl}_2]$, PPh_3 , NEt_3 , toluene, 100 °C, 3 days, 97%; g) K_2CO_3 , MeOH/THF 1:1, 25 °C, 2 h, 98%.

be removed cleanly by column chromatography because of the large differences of their chromatographic mobilities. The complete removal of ethyl 3,5-dihydroxybenzoate and the unreacted starting material was of utmost importance here. The presence of a tiny amount of such contaminants carried through the rest of the synthesis would result in the formation of an inseparable monofunctional polymer chain stopper, a trifunctional or even a tetrafunctional dendrimer cross-linker. Treatment of compound **8** with 4-iodobenzyl bromide (1.1 equiv) in the presence of K_2CO_3 and [18]crown-6 in refluxing acetone afforded the unsymmetrical dendron **9** in 97% yield. No C-alkylation products were found under the reaction conditions. The focal point ethyl ester functionality was then transformed into the corresponding benzyl bromide **10** in two steps by diisobutylaluminum hydride (DIBAL-H) reduction and bromination (PPh_3 , CBr_4) in 59% yield. Coupling of 2.2 equiv of the bromide **10** with the central hydroquinone core furnished the bifunctional G1 dendrimer I-[**S-G1**]-I in 85% yield under Williamson ether synthesis conditions. The two iodo functional groups were then coupled to $\text{TMSC}\equiv\text{CH}$ (TMS = trimethylsilyl) to give $\text{TMSC}\equiv\text{C}$ -[**S-G1**]- $\text{C}\equiv\text{CTMS}$, followed by removal of the TMS groups using K_2CO_3 in MeOH to produce **S-G1** in 95% overall yield.

Synthesis of the **S-G2** dendrimer began with the known 3,5-dibenzoyloxybenzyl bromide **12**^[7] (Scheme 2). Selective mono-O-alkylation of ethyl 3,5-dihydroxybenzoate **11** with bromide **12** (0.25 equiv) afforded compound **13** in 79% yield (based on compound **12**). Again, it was absolutely necessary to separate a small amount of the di-O-alkylation product (ca. 10%) and the starting material **11** from the target product **13**. Fortunately, this was an easy task because of the very different chromatographic mobilities of the three compounds. Compound **13** was then subjected to a second O-alkylation step with the unsymmetrical G1-dendritic bromide **10** to furnish the monofunctionalized G2-dendron **14** under Williamson conditions in 91% yield. The ethyl ester was then converted into the corresponding benzyl bromide

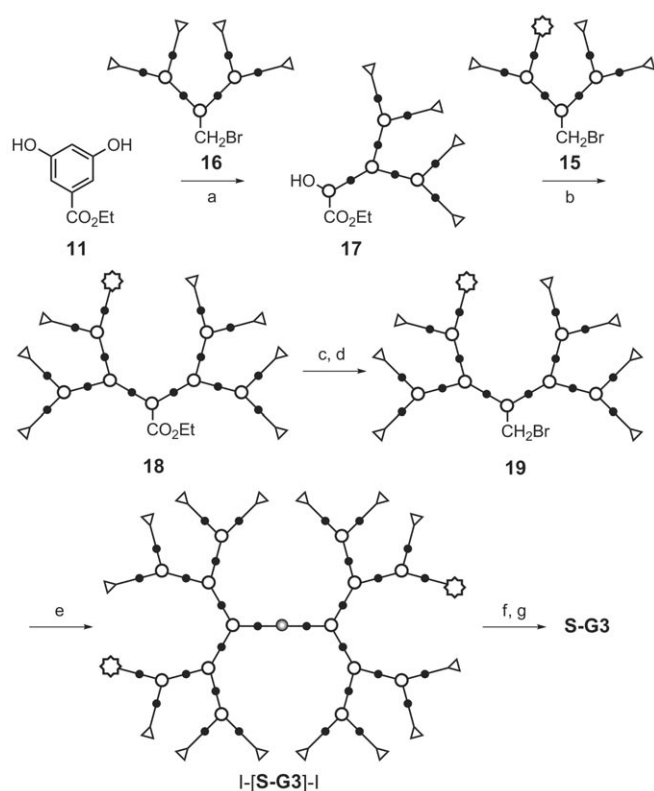


Scheme 2. Synthesis of **S-G2**. Reagents and conditions: a) **12** (0.25 equiv), K_2CO_3 , [18]crown-6, acetone, 56 °C, 12 h, 79%; b) **10** (1.1 equiv), K_2CO_3 , [18]crown-6, acetone, 56 °C, 12 h, 91%; c) DIBAL-H, hexane, $-60\text{ }^\circ\text{C}$ – $0\text{ }^\circ\text{C}$, 2 h, 91%; d) PPh_3 , CBr_4 , THF, 25 °C, 2 h, 87%; e) hydroquinone (0.45 equiv), K_2CO_3 , [18]crown-6, acetone, 56 °C, 3 days, 95%; f) $\text{TMSC}\equiv\text{CH}$, CuI, $[\text{Pd}(\text{PPh}_3)_2\text{Cl}_2]$, PPh_3 , NEt_3 , toluene, 100 °C, 3 days, 94%; g) K_2CO_3 , MeOH/THF 1:1, 25 °C, 2 h, 97%.

mono-O-alkylation (K_2CO_3 , [18]crown-6) of ethyl 3,5-dihydroxybenzoate **11** with the known G2-bromide **16** (0.25 equiv)^[7] to give the hemisubstituted derivative **17** in 64% yield, free of the di-O-alkylation product after chromatography purification (Scheme 3). A second O-alkylation step (K_2CO_3 , [18]crown-6) with the functionalized G2-Br **15** then produced the functionalized G3- CO_2Et dendron **18** in 99% yield. The focal point ester moiety was then converted to afford G3-benzyl bromide **19** derivative in 77% yield by DIBAL-H reduction followed by bromination (CBr_4 , PPh_3). Compound **19** (2.2 equiv) was then secured onto the hydroquinone core to afford the diiodo dendrimer I-[**S-G3**]-I in 95% yield. Palladium-catalyzed coupling of I-[**S-G3**]-I with $\text{TMSC}\equiv\text{CH}$ occurred uneventfully to produce the bis(trimethylsilylacetylene) dendrimer $\text{TMSC}\equiv\text{C}$ -[**S-G3**]- $\text{C}\equiv\text{CTMS}$

15 in two steps as described earlier for compound **9**. The bromide **15** was then anchored to the hydroquinone core to produce the bifunctional dendrimer I-[**S-G2**]-I in 95% yield under Williamson ether synthesis conditions. Finally, the two iodo functional groups were similarly treated to give the target G2 dendrimer **S-G2** by palladium catalyzed coupling with $\text{TMSC}\equiv\text{CH}$ followed by deprotection of the TMS groups with K_2CO_3 in MeOH in 91% overall yield.

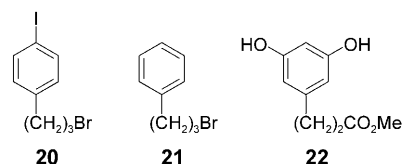
Preparation of the **S-G3** dendrimer involved selective



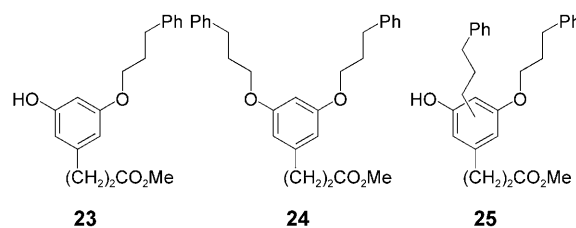
Scheme 3. Synthesis of **S-G3**. Reagents and conditions: a) **16** (0.25 equiv), K_2CO_3 , [18]crown-6, acetone, 56 °C, 12 h, 64%; b) **15** (1.1 equiv), K_2CO_3 , [18]crown-6, acetone, 56 °C, 12 h, 99%; c) DIBAL-H, hexane, $-60^\circ C \rightarrow 0^\circ C$, 2 h, 99%; d) PPh_3 , CBr_4 , THF, 25 °C, 2 h, 78%; e) hydroquinone (0.45 equiv), K_2CO_3 , [18]crown-6, acetone, 56 °C, 3 days, 95%; f) $TMSC\equiv CH$, CuI, $[Pd(PPh_3)_2Cl_2]$, PPh_3 , NEt_3 , toluene, 100 °C, 3 d, 86%; g) TBAF, THF, 25 °C, 15 min, 49%.

in 86% yield. However, removal of the TMS groups in the presence of K_2CO_3 in MeOH (25 °C, 2 h) gave a mixture of the target bifunctional dendrimer **S-G3** together with 10% of some oligomeric Hay homocoupling products^[8] as suggested by 1H NMR spectroscopy and SEC analysis. We suspected that the occurrence of Hay homocoupling was due to a contamination of trace amount of copper salts left over from the previous reaction. Fortunately, this side reaction could be totally suppressed if tetrabutylammonium fluoride (TBAF) was used (20 °C, 15 min) as the deprotecting agent. However, homocoupling products could still be formed if the reaction was left to run for longer than 15 min.

Synthesis of L-Gn dendrimers: Three key intermediates were required for the synthesis of the elongated bifunctional dendrimers **L-Gn**. One was the surface-functionalized iodinated derivative **20**, the second was the commercially available unfunctionalized surface derivative-1-bromo-3-phenylpropane **21**, and the third was the elongated branching agent **22**.^[5] The surface unit **20** could be conveniently prepared from hydrocinnamic acid by using an improved method described in the Supporting Information.



The synthetic routes for the elongated series of dendrimers **L-Gn** were essentially the same as those of the shortened series as shown in Schemes 1–3. Hence, the functionalized dendron was introduced onto the surface of the dendrimer by controlling the reactant stoichiometry during Williamson ether synthesis. However, two notable differences deserve mention: First, the elongated series of compounds possess much better solubility than those of the shortened series. Second, C-alkylation products were formed during the Williamson ether synthesis using the elongated brancher **22**. For example, mono-O-alkylation of brancher **22** with the unfunctionalized surface bromide **21** (0.25 equiv) afforded a mixture of the mono-O-alkylated **23** (77%), di-O-alkylated



24 (13%), and C,O-alkylated **25** (ca. 5%) products. Fortunately, these products could be separated by column chromatography.

Structural characterization: The structures of all compounds were characterized by 1H and ^{13}C NMR spectroscopy. The 1H NMR signals were well separated into different regions and therefore spectral analyses were straightforward. For the **S-Gn** series of compounds, the aromatic signals due to the central hydroquinone core, the brancher, and the surface groups were found at $\delta=6.9$, 6.7–6.4, and 7.5–7.2 ppm, respectively, whereas the benzyl protons originating from the Fréchet-type dendritic branches were found at $\delta=5.0$ –4.8 ppm. For the **L-Gn** series, the presence of the two extra methylene groups on the dendritic branches gave two additional sets of aliphatic proton signals at $\delta=2.8$ –2.6 and 2.2–1.9 ppm, whereas those of the benzyl protons were located at slightly higher field at $\delta=4.0$ –3.8 ppm. The remaining sets of aromatic signals were very similar to those of the **S-Gn** series. Hence, the aromatic signals due to the central hydroquinone core, the brancher, and the surface groups were found at $\delta=6.8$, 6.4–6.2, and 7.4–7.1 ppm, respectively. Depending on the nature of the functionalized surface group, a sharp signal at about $\delta=0.2$ ppm was found for the $TMSC\equiv C$ functionalized compounds, whereas the acetylenic proton signal of the $HC\equiv C$ containing compounds was found at around $\delta=3.0$ ppm.

The ^{13}C NMR spectral features of the synthesized compounds were also consistent with the proposed structures. For the **S-G n** series, the aromatic C signals of the surface, branching, and central core were found to spread within a wide window of $\delta = 160\text{--}100$ ppm, whereas those of the benzylic C atoms were clustered at $\delta = 71\text{--}69$ ppm. For the iodo surface-functionalized compounds, the signal of the aromatic C atoms directly attached to the iodine atom was found at $\delta = 94$ ppm, while two extra acetylenic carbon signals were found for the $\text{TMSC}\equiv\text{C}$ ($\delta = 105$ and 95 ppm) and $\text{HC}\equiv\text{C}$ ($\delta = 84$ and 77 ppm) surface-functionalized compounds. Similarly trends were also observed for the **L-G n** series, except for the presence of aliphatic carbon signals ($\delta = 33\text{--}30$ ppm) belonging to the longer branches.

The purities of the compounds were determined by SEC using polystyrenes as the standards. All compounds gave a sigmoidal peak with a polydispersity index (PDI) of less than 1.03. As expected, the retention times of the fully alkylated dendrons having the same generation number were very close to each other, whereas the bifunctional dendrimers of the same generation possessed slightly shorter retention times. Hence, in the SEC scatter plot of retention time versus theoretical molecular weight (MW), dendrons of the same generation number clustered around each other (Figure 4). Furthermore, the shorter series (**S**) of compounds

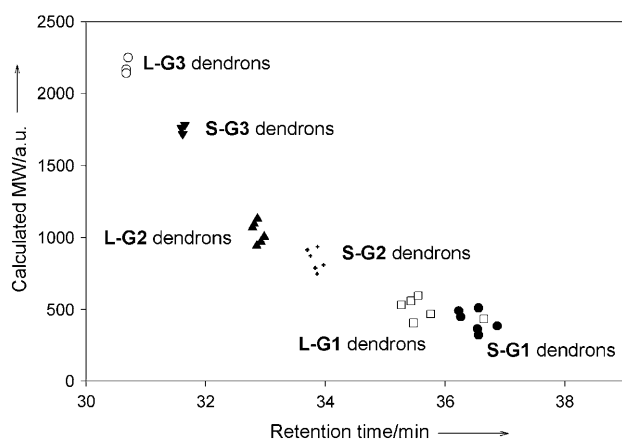


Figure 4. Theoretical MW versus SEC retention time cluster plot of dendrons of various generations.

possessed a longer retention time than the corresponding analogue in the elongated branch series (**L**), indicating that the elongated series of compounds have a slightly larger hydrodynamic radius.

It was mentioned earlier that the presence of a small amount of monofunctional dendrimer could have a detrimental effect on the polymerization efficiency. However, the nearly 100% structural purities of these compounds could not be assessed from the relative integration values of the signals for the functionalized surface versus the unfunctionalized surface groups by ^1H NMR spectroscopy. Mass spectroscopic (MS) analysis, in particular FAB/MALDI-TOF, may provide a better estimate of the structural purities of

the target compounds. For all the iodo-functionalized dendrons, the major signals are the molecular peaks due to $[M]^+$, $[M+H]^+$, $[M+\text{Na}]^+$ or $[M+K]^+$. For example, the MS spectrum of the mono-iodinated G3 dendron **19** gave a base peak signal corresponding to $[M+H]^+$ at m/z 1783.4 (Figure 5). The other minor signals are due to fragmentation

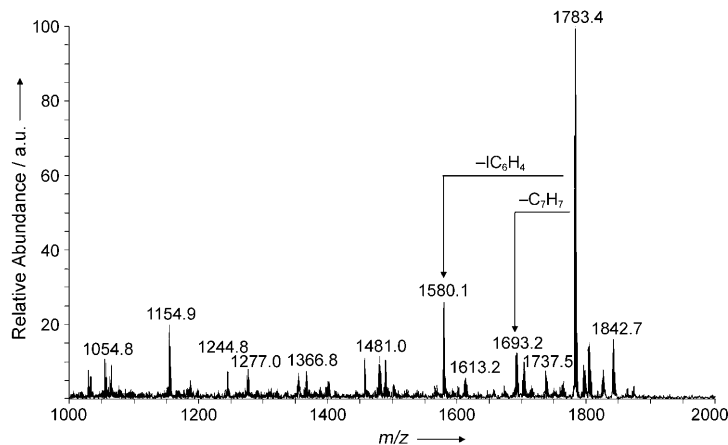
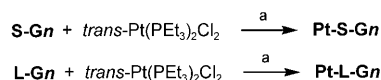


Figure 5. Mass spectrum of mono-iodinated G3 dendron **19**, showing the $M+H^+$ peak at m/z 1783. The M^+ peak of the de-iodinated species has an m/z value of 1657.

ions. However, we could not find the signal due to the corresponding de-iodinated dendron that could potentially be formed during DIBAL-H reduction of the corresponding G3 ester dendron **18**.

Copolymerization studies: Having obtained the target bifunctional dendrimers, we decided to find out the optimized conditions to carry out their 1:1 copolymerizations with the platinum linker *trans*-[Pt(PET₃)₂Cl₂] in the presence of CuI and diisopropylamine in CHCl₃ at 40°C. With **S-G1** as the model substrate, the copolymerization was conducted under different monomer concentrations of 4.4, 8.7, and 17 mM. It was found that at low concentration (4.4 mM), the product contained a significant amount of low molecular weight (LMW) cyclic oligomers (see below) as determined by SEC and MS analyses (see the Supporting Information for details). The amount of LMW oligomers was much less when the polymerizations were conducted at 8.7 and 17 mM. However, owing to the much larger MW of the G3 monomers, their copolymerizations at 17 mM resulted in a very viscous solution, which significantly reduced the stirring efficiency. Hence, all copolymerizations were carried out at 8.7 mM at 40°C under a closed system to prevent solvent evaporation.

The copolymerizations of the two series of bifunctional dendrimers were then conducted side by side under identical reaction conditions to evaluate the structural effect on the formation of poly(dendrimer)s (Scheme 4). After polymerization, the yellow products **Pt-S-G n** and **Pt-L-G n** were isolated by passing them through a short column of alumina followed by solvent evaporation, and they were then sub-



Scheme 4. Copolymerizations of **S-Gn** and **L-Gn** with *trans*-[Pt-(PEt₃)₂Cl₂]. Reagents and conditions: a) CuI, HNPr₂, CHCl₃, 40 °C, 72 h.

jected to ¹H, ¹³C, and ³¹P NMR spectroscopic characterization. For example, the ¹H NMR spectrum of **Pt-S-G2** revealed the complete disappearance of the acetylenic proton signals (δ = 3.07 ppm) and the upfield shifting of the aromatic signals *ortho* to the functional 4-ethynylphenyl surface moieties (Figure 6). Furthermore, the signals due to the tri-

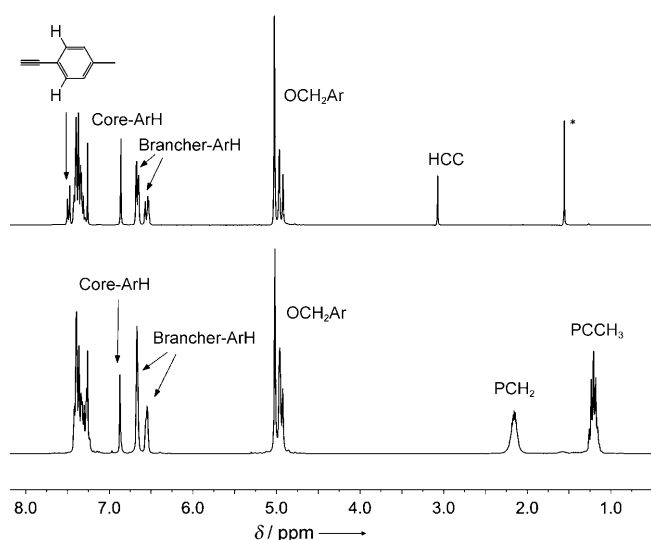


Figure 6. ¹H NMR spectra (300 MHz, CDCl₃) of **S-G2** (top) and **Pt-S-G2** (bottom). The signal labeled with an asterisk is due to residual H₂O.

ethylphosphine ligands (δ = 2.25–2.10 and 1.26–1.10 ppm) attached to the platinum metal could also be found. The ³¹P{¹H} NMR spectra exhibited one major ³¹P peak located at δ = 11.1 ppm with two ¹⁹⁵Pt satellite signals [¹J(Pt,P) ≈ 2360 Hz] of one sixth intensity (Figure 7). For the higher generation G3 poly(dendrimer)s **Pt-S-G3** and **Pt-L-G3**, minor peaks at δ = 8.6 and 14.9 ppm were also observed, suggesting that the polymerizations were of lower efficiency.

The molecular weights (*M_w*) and distributions of the poly(dendrimer)s were determined by SEC and static and dynamic laser light scattering (LLS) studies (Table 1 and Figure 8). Because of the formation of poly(dendrimer) aggregates in concentrated THF and also in concentrated toluene solutions, their *M_w* values, apart from for **Pt-S-G2** and **Pt-S-G3**, could not be accurately determined by LLS (see then Supporting Information for details). Hence, the tabulated DP values are based on the *M_w* value obtained from SEC calculations. Aggregate formation was not found in SEC measurements as they were carried out with highly diluted solutions in THF. It should also be noted that polystyrenes were used as standards and hence the calculated *M_w*

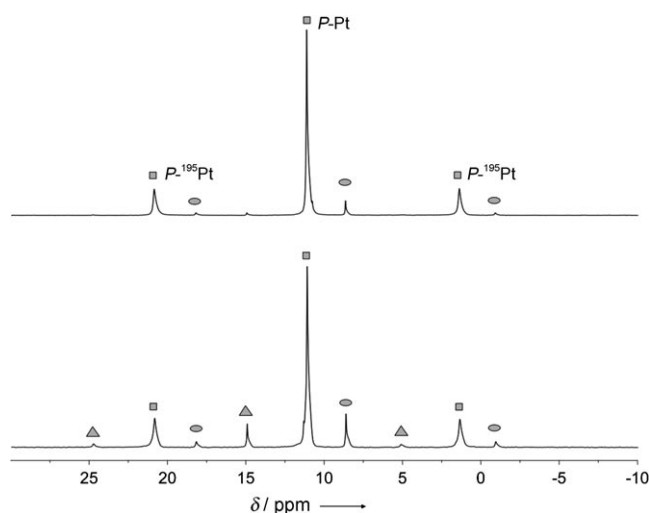


Figure 7. ³¹P{¹H} NMR spectra (122 MHz, CDCl₃) of **Pt-S-G2** (top), showing two sets of ³¹P signals (square and eclipse), and **Pt-S-G3** (bottom), showing three sets of ³¹P signals (square, eclipse, and triangle).

Table 1. SEC (40 °C) and LLS data (25 °C) of poly(dendrimer)s in THF.

Sample	SEC <i>M_w</i> × 10 ⁻³	DP ^[a]	PDI ^[a]	% of LMW oligomers ^[a,b]	LLS <i>M_w</i> × 10 ⁻³
Pt-S-G1	40	34	1.9	1	— ^[c]
Pt-L-G1	53	39	1.9	2	— ^[c]
Pt-S-G2	122	60	2.3	<0.2	71
Pt-L-G2	55	22	1.6	4	— ^[c]
Pt-S-G3	79	21	1.8	3	64
Pt-L-G3	86	19	1.6	14	— ^[c]

[a] Values calculated from SEC data; [b] wt% up to the pentamer; [c] *M_w* value of the non-aggregated poly(dendrimer) could not be determined accurately by LLS because of the relatively large intensity of the aggregated peak.

values might deviate significantly from the actual figures. Nonetheless, the conclusions drawn below regarding to the relative polymerization efficiencies of these two series are still valid. Because of the step-growth nature of the polymerization, the polydispersity index (PDI) values were close to 2. However, several interesting findings are noteworthy. First, a significant amount (0.2–14% by weight) of low molecular weight (LMW) oligomers (calculated up to the pentamer) was found. Initially we thought that these were the partially reacted open-chain oligomers still bearing either free acetylene or Pt–Cl chain ends. However, subjecting the polymer mixture to further reaction did not result in a decrease in the signal intensities of such LMW oligomeric peaks. Most interestingly, apart from the SEC trace of the products from **S-G1**, the rest of the SEC traces showed the presence of a peak (labeled with an asterisk in Figure 8) that possessed a longer retention time than that of the corresponding dendritic macromonomer. Hence, such peaks most likely arose from the cyclic monomer. Indeed, this was confirmed by the MS data of the purified samples by preparative SEC. For example, for the SEC trace of **Pt-L-G1**, the signal peak with retention time of 33 min had a molecular

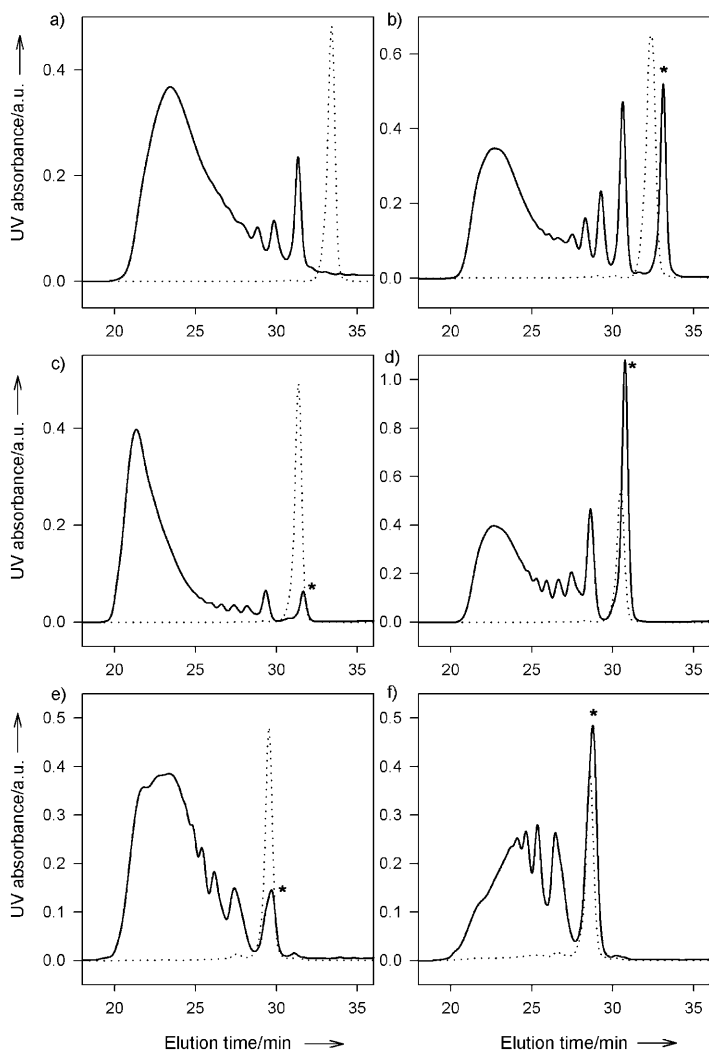
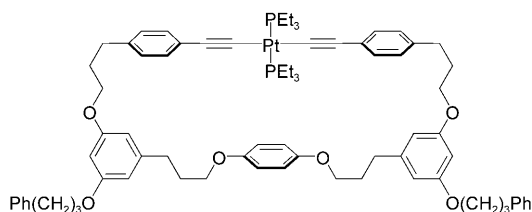


Figure 8. SEC chromatograms of a) **Pt-S-G1**, b) **Pt-L-G1**, c) **Pt-S-G2**, d) **Pt-L-G2**, e) **Pt-S-G3**, and f) **Pt-L-G3** (solid lines). The peaks labeled with an asterisk are cyclic monomer peaks. The dotted lines are the SEC traces of the corresponding dendritic macromonomers. The wt% of the oligomers is exaggerated in these plots as the x axis is on a logarithmic scale of polymer MW.

peak at m/z 1361.6254, which corresponded to the structure of the cyclic monomer **26** (see the Supporting Information for MS data of cyclic monomers of other poly(dendrimer)s).

The second point worth mentioning is that the amount of LMW oligomers of the **S-Gn** series was less than that of the



26 Theoretical $M+H^+$: 1361.6269

L-Gn series, suggesting that more cyclic oligomers were formed from the **L-Gn** series. This difference was more pronounced for the G3 compounds, for which 3% of LMW oligomers was found for the **S** series, in contrast to 14% for the **L** series. This finding revealed a hitherto unknown factor in the polymerization of macromonomers with two remote reactive functionalities separated at a distance, namely, that structurally more flexible monomers are more prone to undergo cyclization than linear propagation relative to their rigid analogues.

Our third observation was that the polymerization efficiency within the same series of dendrimers was strongly dependent on the dendrimer generation. Both the G1 and G2 dendrimers polymerized with a larger DP value than the G3 dendrimers. The drop of the DP values for the G3 poly(dendrimer)s could be attributed to the increased steric inhibition during polymerization, and also to the lowering of surface density of the acetylenic moiety (from 1/2 of G1 dendrimers to 1/8 of the G3 dendrimers). A comparison of the SEC calculated DP values (19–60) in the current study to those (20–63 based on SEC data) obtained in our previous study^[5] involving elongated C-10 bifunctional macromonomers **1** suggested that having a protruding $C\equiv CH$ reactive functionality sticking up from the dendrimer surface did not possess any obvious advantage in terms of polymerization efficiency. As the SEC calculated M_w values were known to be grossly underestimated by polystyrene standards,^[9] the actual DP values of such poly(dendrimer)s could be very high. Unfortunately, we were unable to extract reliable M_w data from static or dynamic LLS studies to support this claim.

Conclusion

In summary, we report herein the controlled syntheses of surface bifunctional dendrimers **S-Gn** and **L-Gn** by a convergent synthetic strategy. Such dendritic macromonomers were used to copolymerize with $trans$ -[Pt(PEt₃)₂Cl₂] to produce the corresponding poly(dendrimer)s **Pt-S-Gn** and **Pt-L-Gn**, respectively. The polymerization efficiency was found to depend on the monomer concentration. In general, lower monomer concentration led to the formation of more cyclic oligomers. It was also revealed that the structurally more rigid **S-Gn** series underwent polymer propagation to form linear poly(dendrimer)s much more effectively. In contrast, the structurally more flexible **L-Gn** series had a relatively higher tendency to form cyclic oligomers. Furthermore, the presumed advantage of protruding the reactive functional group out of the dendrimer surface to improve the polymerization efficiency could not be substantiated in this investigation. Our studies revealed that there are additional structural factors that are not encountered in the polymerization of conventional small monomers are involved in the polymerization of such macromonomers.

Experimental Section

I-[S-G1]-I: A mixture of hydroquinone (0.803 g, 7.29 mmol), bromide **10** (8.17 g, 16.0 mmol), Cs₂CO₃ (8.32 g, 25.5 mmol), and dibenzo-[24]crown-8 (5 mg) in DMF (40 mL) was stirred under N₂ at 25 °C for 12 h. The reaction mixture was filtered and washed with CH₂Cl₂. The filtrates were combined, dried in vacuo, and purified by flash chromatography (eluent: hexane/CHCl₃ 1:1) to give the target compound (5.98 g, 85%) as a white solid. M.p. 136.5–137.5 °C; *R*_f = 0.30 (hexane/CHCl₃ 1:1); ¹H NMR (300 MHz, CDCl₃): δ = 7.71 (d, ³*J*(H,H) = 8.4 Hz, 4H; ArH), 7.29–7.48 (m, 10H; ArH), 7.16 (d, ³*J*(H,H) = 8.4 Hz, 4H; ArH), 6.88 (s, 4H; core-ArH), 6.70 (s, 2H; ArH), 6.66 (s, 2H; ArH), 6.54 (t, ³*J*(H,H) = 2.1 Hz, 2H; ArH), 5.04 (s, 4H; ArCH₂O), 4.98 (s, 4H; ArCH₂O), 4.96 ppm (s, 4H; ArCH₂O); ¹³C NMR (75 MHz, CDCl₃): δ = 160.2, 159.9, 153.1, 139.9, 137.7, 136.8, 136.6, 129.4, 128.7, 128.1, 127.6, 115.9, 106.5, 106.3, 101.5, 93.6, 70.5, 70.1, 69.4 ppm; MS (EI): *m/z* (%): 966 (<1) [*M*⁺]; HRMS (EI) calcd for C₄₈H₄₀O₆: 966.0909; found: 966.0913.

I-[S-G2]-I: A mixture of hydroquinone (0.16 g, 1.46 mmol), bromide **14** (3.00 g, 3.21 mmol), K₂CO₃ (0.61 g, 4.38 mmol), and [18]crown-6 (2 mg) in acetone (80 mL) was heated to reflux for 3 days. The mixture was filtered and washed with CH₂Cl₂. The combined filtrates were evaporated in vacuo and the residue was chromatographed on silica gel to give the product (2.52 g, 95%) as a white foam (eluent: hexane/CH₂Cl₂ 1:2 to CH₂Cl₂). *R*_f = 0.33 (hexane/CH₂Cl₂ 1:2); ¹H NMR (300 MHz, CDCl₃): δ = 7.68 (d, ³*J*(H,H) = 8.1 Hz, 4H; ArH), 7.27–7.47 (m, 30H; ArH), 7.14 (d, ³*J*(H,H) = 8.4 Hz, 4H; ArH), 6.86 (s, 4H; core-ArH), 6.66–6.71 (m, 6H; ArH), 6.60–6.66 (m, 6H; ArH), 6.57 (t, ³*J*(H,H) = 2.1 Hz, 2H; ArH), 6.53 (t, ³*J*(H,H) = 2.1 Hz, 4H; ArH), 5.03 (s, 12H; PhCH₂O), 4.97 (s, 4H; ArCH₂O), 4.96 (s, 8H; ArCH₂O), 4.92 ppm (s, 4H; ArCH₂O); ¹³C NMR (75 MHz, CDCl₃): δ = 160.1, 160.0, 159.9, 159.8, 153.0, 139.8, 139.3, 139.2, 137.5, 136.73, 136.68, 136.4, 129.3, 128.5, 128.0, 127.5, 115.7, 106.4, 106.3, 101.5, 93.5, 70.3, 69.9, 69.83, 69.77, 69.2 ppm; MS (ESI): *m/z* (%): 1816 (100) [*M*+H⁺]; HRMS (ESI) calcd for C₁₀₄H₈₈I₂O₁₄+H⁺: 1815.4336; found: 1815.4327; elemental analysis calcd (%) for C₁₀₄H₈₈I₂O₁₄: C 68.80, H 4.89; found: C 68.76, H 4.56, N < 0.10.

I-[S-G3]-I: A mixture of hydroquinone (13.6 mg, 0.124 mmol), bromide **19** (484 mg, 0.272 mmol), K₂CO₃ (51.2 mg, 0.371 mmol), and [18]crown-6 (2 mg) in acetone (10 mL) was heated to reflux for 3 days. The mixture was filtered and washed with CH₂Cl₂. The combined filtrates were concentrated in vacuo and the residue was chromatographed on silica gel to give the product (412 mg, 95%) as a colorless oil (eluent: hexane/CH₂Cl₂ 1:1 to CH₂Cl₂ to CH₂Cl₂/Et₂O 100:1). *R*_f = 0.52 (hexane/CH₂Cl₂ 1:2); ¹H NMR (300 MHz, CDCl₃): δ = 7.67 (d, ³*J*(H,H) = 8.1 Hz, 4H; ArH), 7.27–7.48 (m, 70H; ArH), 7.12 (d, ³*J*(H,H) = 8.1 Hz, 4H; ArH), 6.85 (s, 4H; core-ArH), 6.61–6.74 (m, 28H; ArH), 6.49–6.61 (m, 14H; ArH), 5.01 (s, 28H; PhCH₂O), 4.95 (s, 24H; ArCH₂O), 4.93 (s, 4H; ArCH₂O), 4.89 ppm (s, 4H; ArCH₂O); ¹³C NMR (75 MHz, CDCl₃): δ = 160.2, 160.14, 160.11, 160.09, 159.9, 153.2, 139.9, 139.41, 139.39, 139.36, 139.3, 137.7, 136.9, 136.8, 136.6, 129.4, 128.7, 128.1, 128.0, 127.6, 115.9, 106.6, 106.5, 106.4, 101.7, 93.6, 70.5, 70.1, 70.0, 69.4 ppm; HRMS (MALDI-TOF) calcd for C₂₁₆H₁₈₄I₂O₃₀+Na⁺: 3536.0921; found: 3536.1139; elemental analysis calcd (%) for C₂₁₆H₁₈₄I₂O₃₀: C 73.84, H 5.28; found: C 73.64, H 5.21, N < 0.10.

General procedure for the synthesis of TMSC≡C-[S-Gn]-C≡CTMS: A mixture of I-[S-Gn]-I (1.0 equiv), [(PPh₃)₂PdCl₂] (0.5 equiv), PPh₃ (0.5 equiv), CuI (0.5 equiv), trimethylsilylacetylene (15 equiv), and Et₃N (15 equiv) in toluene was frozen in a sealed tube by liquid N₂ and degassed with N₂ (3 times). The mixture was allowed to warm to 25 °C and then heated at 100 °C for 3 days. After the reaction was completed, Et₂O was added and the reaction mixture was filtered. The filtrate was dried in vacuo and purified by flash column chromatography to give the target compound.

TMSC≡C-[S-G1]-C≡CTMS: Starting from I-[S-G1]-I (610 mg, 0.63 mmol), [(PPh₃)₂PdCl₂] (220 mg, 0.32 mmol), PPh₃ (83 mg, 0.32 mmol), CuI (60 mg, 0.32 mmol), trimethylsilylacetylene (1.34 mL, 0.95 mmol), and Et₃N (1.32 mL, 0.95 mmol) in toluene (20 mL), the product (556 mg, 97%) was obtained as a pale yellow foam after flash chromatography (eluent: hexane/EtOAc 8:1). *R*_f = 0.24 (hexane/EtOAc 8:1);

¹H NMR (300 MHz, CDCl₃): δ = 7.47 (d, ³*J*(H,H) = 8.1 Hz, 4H; ArH), 7.28–7.44 (m, 14H; ArH), 6.87 (s, 4H; core-ArH), 6.68 (s, 2H; ArH), 6.65 (s, 2H; ArH), 6.53 (t, ³*J*(H,H) = 2.1 Hz, 2H; ArH), 5.03 (s, 4H; ArCH₂O), 5.02 (s, 4H; ArCH₂O), 4.95 (s, 4H; ArCH₂O), 0.25 ppm (s, 18H; Si(CH₃)₃); ¹³C NMR (75 MHz, CDCl₃): δ = 160.2, 160.0, 153.2, 139.9, 137.4, 136.8, 132.3, 128.7, 128.1, 127.7, 127.2, 122.8, 115.9, 106.5, 106.4, 104.9, 101.6, 94.6, 70.6, 70.2, 69.7, 0.1 ppm; MS (ESI): *m/z* (%): 929 (100) [*M*+Na⁺]; HRMS (ESI) calcd for C₅₈H₅₈O₆Si₂+Na⁺: 929.3664; found: 929.3680; elemental analysis calcd (%) for C₅₈H₅₈O₆Si₂: C 76.78, H 6.44; found: C 76.43, H 6.11, N < 0.10.

TMSC≡C-[S-G2]-C≡CTMS: Starting from I-[S-G2]-I (408 mg, 0.22 mmol), [(PPh₃)₂PdCl₂] (79 mg, 0.11 mmol), PPh₃ (29 mg, 0.11 mmol), CuI (21 mg, 0.11 mmol), trimethylsilylacetylene (0.48 mL, 3.37 mmol), and Et₃N (0.47 mL, 3.37 mmol) in toluene (10 mL), the product (369 mg, 94%) was obtained as a pale yellow foam after flash chromatography (eluent: hexane/CH₂Cl₂ 4:5 to CH₂Cl₂). *R*_f = 0.54 (hexane/CH₂Cl₂ 2:3); ¹H NMR (300 MHz, CDCl₃): δ = 7.47 (d, ³*J*(H,H) = 7.8 Hz, 4H; ArH), 7.27–7.45 (m, 34H; ArH), 6.88 (s, 4H; core-ArH), 6.68–6.72 (m, 6H; ArH), 6.61–6.68 (m, 6H; ArH), 6.58 (t, ³*J*(H,H) = 2.1 Hz, 2H; ArH), 6.50–6.56 (m, 4H; ArH), 5.03 (s, 12H; PhCH₂O), 5.02 (s, 4H; ArCH₂O), 4.98 (s, 4H; ArCH₂O), 4.97 (s, 4H; ArCH₂O), 4.93 (s, 4H; ArCH₂O), 0.27 ppm (s, 18H; Si(CH₃)₃); ¹³C NMR (75 MHz, CDCl₃): δ = 160.1, 160.0, 159.9, 153.1, 139.8, 139.3, 137.3, 136.8, 132.1, 128.6, 128.0, 127.6, 127.2, 122.7, 115.8, 106.4, 105.0, 101.6, 94.5, 70.4, 70.0, 69.9, 69.5, 0.1 ppm; MS (ESI): *m/z* (%): 1756 (75) [*M*+H⁺]; HRMS (ESI) calcd for C₁₁₄H₁₀₆O₁₄Si₂+H⁺: 1755.7194; found: 1755.7201; elemental analysis calcd (%) for C₁₁₄H₁₀₆O₁₄Si₂: C 77.96, H 6.08; found: C 77.69, H 5.96, N < 0.10.

TMSC≡C-[S-G3]-C≡CTMS: Starting from I-[S-G3]-I (346 mg, 0.098 mmol), [(PPh₃)₂PdCl₂] (79 mg, 0.049 mmol), PPh₃ (29 mg, 0.049 mmol), CuI (21 mg, 0.049 mmol), trimethylsilylacetylene (0.48 mL, 1.48 mmol), and Et₃N (0.47 mL, 1.48 mmol) in toluene (3.5 mL), the product (294 mg, 86%) was obtained as a pale yellow foam after flash chromatography (eluent: hexane/CH₂Cl₂ 1:2 to CH₂Cl₂ to CH₂Cl₂/Et₂O 100:1). *R*_f = 0.46 (hexane/CH₂Cl₂ 1:2); ¹H NMR (300 MHz, CDCl₃): δ = 7.45 (d, ³*J*(H,H) = 8.4 Hz, 4H; ArH), 7.27–7.42 (m, 74H; ArH), 6.83 (s, 4H; core-ArH), 6.59–6.71 (m, 28H; ArH), 6.55 (t, ³*J*(H,H) = 2.1, 8H; ArH), 6.48–6.54 (m, 6H; ArH), 4.99 (s, 28H; PhCH₂O), 4.98 (s, 4H; ArCH₂O), 4.94 (s, 24H; ArCH₂O), 4.88 (s, 4H; ArCH₂O), 0.25 ppm (s, 18H; Si(CH₃)₃); ¹³C NMR (75 MHz, CDCl₃): δ = 160.2, 160.14, 160.05, 160.0, 159.9, 153.1, 139.8, 139.32, 139.26, 137.3, 136.82, 136.79, 136.76, 132.1, 128.6, 128.0, 127.6, 127.2, 122.7, 115.8, 106.4, 105.0, 101.6, 94.5, 70.4, 70.0, 69.9, 69.5, 0.0 ppm; HRMS (MALDI-TOF) calcd for C₂₂₆H₂₀₂O₃₀Si₂+Na⁺: 3476.3774; found: 3476.3867; elemental analysis calcd (%) for C₂₂₆H₂₀₂O₃₀Si₂: C 78.58, H 5.89; found: C 78.37, H 5.83, N < 0.10.

S-G1: A mixture of TMSC≡C-[S-G1]-C≡CTMS (320 mg, 0.35 mmol) and K₂CO₃ (240 mg, 1.76 mmol) in THF/MeOH (v/v 1:1, 20 mL) was stirred at 25 °C for 2 h. The reaction mixture was filtered and washed with CH₂Cl₂. The combined filtrates were dried in vacuo and purified by flash column chromatography to give the target product (265 mg, 98%) as a colorless oil after flash chromatography (eluent: hexane/CH₂Cl₂ 1:1 to CH₂Cl₂ to CH₂Cl₂/Et₂O 100:1). *R*_f = 0.53 (hexane/CH₂Cl₂ 1:4); ¹H NMR (300 MHz, CDCl₃): δ = 7.51 (d, ³*J*(H,H) = 8.1 Hz, 4H; ArH), 7.29–7.46 (m, 14H; ArH), 6.87 (s, 4H; core-ArH), 6.69 (s, 2H; ArH), 6.66 (s, 2H; ArH), 6.55 (t, ³*J*(H,H) = 2.1 Hz, 2H; ArH), 5.04 (s, 8H; PhCH₂O+ArCH₂O), 4.95 (s, 4H; ArCH₂O), 3.09 ppm (s, 2H; C=CH); ¹³C NMR (75 MHz, CDCl₃): δ = 160.3, 160.0, 153.1, 140.0, 137.7, 136.8, 132.5, 128.7, 128.2, 127.7, 127.4, 121.8, 115.9, 106.5, 106.4, 101.6, 83.5, 77.6, 70.6, 70.2, 69.6 ppm; MS (ESI): *m/z* (%): 763 (100) [*M*+H⁺]; HRMS (ESI) calcd for C₅₂H₄₂O₆+H⁺: 763.3054; found: 763.3060; elemental analysis calcd (%) for C₅₂H₄₂O₆: C 81.87, H 5.55; found: C 82.25, H 5.63, N < 0.10.

S-G2: A mixture of TMSC≡C-[S-G2]-C≡CTMS (701 mg, 0.40 mmol) and K₂CO₃ (280 mg, 2.00 mmol) in THF/MeOH (v/v 1:1, 10 mL) was stirred at 25 °C for 2 h. The reaction mixture was filtered and washed with CH₂Cl₂. The combined filtrates were dried in vacuo and purified by flash column chromatography to give the target compound (623 mg, 97%) as a white foam after flash chromatography (eluent: hexane/

CH₂Cl₂ 1:2 to CH₂Cl₂ to CH₂Cl₂/Et₂O 100:1). $R_f=0.29$ (hexane/CH₂Cl₂ 1:2); ¹H NMR (300 MHz, CDCl₃): $\delta=7.49$ (d, ³J(H,H)=8.4 Hz, 4H; ArH), 7.27–7.45 (m, 34H; ArH), 6.86 (s, 4H; core-ArH), 6.67–6.71 (m, 6H; ArH), 6.61–6.67 (m, 6H; ArH), 6.57 (t, ³J(H,H)=2.1 Hz, 2H; ArH), 6.49–6.56 (m, 4H; ArH), 5.02 (s, 16H; PhCH₂O+ArCH₂O), 4.97 (s, 8H; ArCH₂O), 4.92 (s, 4H; ArCH₂O), 3.07 ppm (s, 2H; C≡CH); ¹³C NMR (75 MHz, CDCl₃): $\delta=160.2$, 160.12, 160.08, 160.0, 153.2, 139.9, 139.4, 139.3, 137.7, 136.9, 136.8, 132.4, 128.7, 128.1, 127.7, 127.3, 121.8, 115.9, 106.6, 106.5, 106.4, 101.69, 101.66, 101.6, 83.5, 77.6, 70.6, 70.2, 70.04, 69.98, 69.6 ppm; MS (ESI): m/z (%): 1612 (100) [M+H⁺]; HRMS (MALDI-TOF) calcd for C₁₀₈H₉₀O₁₄+Na⁺: 1634.6257; found: 1634.6292; elemental analysis calcd (%) for C₁₀₈H₉₀O₁₄: C 80.48, H 5.63; found: C 80.10, H 5.30, N <0.10.

S-G3: A mixture of TMSC≡C-[S-G3]-C≡CTMS (357 mg, 10.3 mmol) and TBAF (1.0 M in THF, 0.3 mL) in THF (10 mL) was stirred at 25 °C for 15 min. The reaction mixture was filtered and washed with CH₂Cl₂. The combined filtrates were dried in vacuo and purified by flash column chromatography to give the target compound (169 mg, 49%) as a pale yellow foam after flash column chromatography (eluent: hexane/CH₂Cl₂ 1:1 to CH₂Cl₂ to CH₂Cl₂/Et₂O 50:1). $R_f=0.39$ (hexane/CH₂Cl₂ 1:3); ¹H NMR (300 MHz, CDCl₃): $\delta=7.46$ (d, ³J(H,H)=8.4 Hz, 4H; ArH), 7.27–7.43 (m, 74H; ArH), 6.82 (s, 4H; core-ArH), 6.59–6.73 (m, 28H; ArH), 6.46–6.59 (m, 14H; ArH), 4.99 (s, 32H; PhCH₂O+ArCH₂O), 4.94 (s, 24H; ArCH₂O), 4.87 (s, 4H; ArCH₂O), 3.06 ppm (s, 2H; C≡CH); ¹³C NMR (75 MHz, CDCl₃, one of the C≡C signals was too weak to be observed): $\delta=160.3$, 160.2, 160.1, 160.0, 153.2, 139.9, 139.4, 139.3, 137.7, 136.9, 136.8, 132.4, 128.7, 128.1, 127.7, 127.4, 121.8, 115.9, 106.5, 101.7, 83.5, 70.6, 70.2, 70.1, 69.6 ppm; HRMS (MALDI-TOF) calcd for C₂₂₀H₁₈₆O₃₀+Na⁺: 3332.2988; found: 3332.2790; elemental analysis calcd (%) for C₂₂₀H₁₈₆O₃₀: C 79.83, H 5.66; found: C 79.77, H 5.66.

General procedure for the synthesis of poly(dendrimer)s Pt-S-Gn and Pt-L-Gn:

A mixture of the S-Gn or L-Gn dendrimers (1.0 equiv, 8.7 mmol), *trans*-[Pt(PEt₃)₂Cl₂] (1.0 equiv) in CHCl₃/iPr₂NH (v/v 1:1) was frozen in a sealed tube by liquid N₂ and degassed with N₂ (3 times). The mixture was allowed to warm to 25 °C followed by the addition of CuI (0.5 equiv). The mixture was then heated at 40 °C for 2 days. The solvent was concentrated in vacuo, the residue was dissolved in a minimum amount of CHCl₃ and filtered through a short pad of alumina, and the target poly(dendrimer) was isolated by precipitation in MeOH.

Pt-S-G1: Starting from S-G1 (100 mg, 0.131 mmol), *trans*-[Pt(PEt₃)₂Cl₂] (65.8 mg, 0.131 mmol), and CuI (12.5 mg, 0.066 mmol) in CHCl₃/iPr₂NH (v/v 1:1, 15 mL), the polymer (148 mg, 95%; 107 mg, 69% after precipitation) was obtained as a yellow powder. ¹H NMR (300 MHz, CDCl₃): $\delta=7.15$ –7.55 (m, 18H; ArH), 6.89 (s, 4H; core-ArH), 6.67 (s, 4H; ArH), 6.55 (s, 2H; ArH), 5.03 (s, 4H; ArCH₂O), 4.97 (s, 4H; ArCH₂O), 4.95 (s, 4H; ArCH₂O), 1.97–2.31 (m, 12H; PCH₂), 1.03–1.37 ppm (m, 18H; PCH₂CH₃); ¹³C NMR (75 MHz, CDCl₃): $\delta=160.23$, 160.16, 153.1, 139.8, 136.8, 133.3, 131.1, 128.6, 128.1, 127.6, 127.5, 115.8, 109.3 (C≡Cpt), 108.4 (t, ²J(C,P)=14.3 Hz; C≡Cpt), 106.4, 106.3, 101.5, 70.6, 70.1, 16.4 (quintet like, ¹J(C,P)=17.5 Hz; PCH₂), 8.4 ppm; ³¹P NMR (122 MHz, CDCl₃): δ =(major peak): 11.1 (¹J(Pt,P)=2370 Hz); (minor peaks): 14.9 (¹J(Pt,P)=2390 Hz), 8.6 ppm (¹J(Pt,P)=2320 Hz).

Pt-S-G2: Starting from S-G2 (211 mg, 0.131 mmol), *trans*-[Pt(PEt₃)₂Cl₂] (65.8 mg, 0.131 mmol), and CuI (12.5 mg, 0.066 mmol) in CHCl₃/iPr₂NH (v/v 1:1, 15 mL), the product (236 mg, 88%; 218 mg, 81% after precipitation) was obtained as a yellow powder. ¹H NMR (300 MHz, CDCl₃): $\delta=7.17$ –7.51 (m, 38H; ArH), 6.87 (s, 4H; core-ArH), 6.67 (s, 12H; ArH); 6.49–6.60 (m, 6H; ArH), 5.02 (s, 12H; ArCH₂O), 4.96 (s, 12H; ArCH₂O), 4.93 (s, 4H; ArCH₂O), 1.97–2.31 (m, 12H; PCH₂), 1.08–1.32 ppm (m, 18H; PCH₂CH₃); ¹³C NMR (75 MHz, CDCl₃): $\delta=160.2$, 160.1, 153.1, 139.8, 139.3, 132.1, 136.8, 133.3, 131.0, 128.6, 128.0, 127.6, 127.5, 115.8, 109.3 (C≡Cpt), 108.4 (t, ²J(C,P)=14.3 Hz; C≡Cpt), 106.4, 101.6, 70.5, 70.1, 16.4 (quintet like, ¹J(C,P)=17.5 Hz; PCH₂), 8.4 ppm; ³¹P NMR (122 MHz, CDCl₃): δ =(major peak): 11.2 (¹J(Pt,P)=2370 Hz); (minor peak): 8.7 (¹J(Pt,P)=2320 Hz).

Pt-S-G3: Starting from S-G3 (155 mg, 0.047 mmol), *trans*-[Pt(PEt₃)₂Cl₂] (23.5 mg, 0.047 mmol), and CuI (4.5 mg, 0.023 mmol) in CHCl₃/iPr₂NH (v/v 1:1, 5.4 mL), the product (173 mg, 99%; 162 mg, 93% after precipi-

tation) was obtained as a yellow powder. ¹H NMR (300 MHz, CDCl₃): $\delta=7.15$ –7.47 (m, 78H; ArH), 6.84 (s, 4H; core-ArH), 6.66 (brs, 28H; ArH), 6.55 (brs, 14H; ArH), 4.99 (s, 32H; ArCH₂O), 4.94 (s, 24H; ArCH₂O), 4.88 (s, 4H; ArCH₂O), 1.95–2.39 (m, 12H; PCH₂), 1.05–1.38 ppm (m, 18H; PCH₂CH₃); ¹³C NMR (75 MHz, CDCl₃): $\delta=160.2$, 160.1, 153.1, 139.8, 139.31, 139.26, 139.2, 136.8, 133.3, 131.1, 128.6, 128.1, 127.6, 127.5, 115.8, 109.4 (C≡Cpt), 108.4 (C≡Cpt, weak signal), 106.4, 101.6, 70.5, 70.1, 70.0, 16.4 (quintet like, ¹J(C,P)=17.7 Hz; PCH₂), 8.4 ppm; ³¹P NMR (122 MHz, CDCl₃): δ =(major peak): 11.1 (¹J(Pt,P)=2370 Hz); (minor peaks): 14.9 (¹J(Pt,P)=2380 Hz), 8.6 ppm (¹J(Pt,P)=2320 Hz).

Pt-L-G1: Starting from L-G1 (122 mg, 0.131 mmol), *trans*-[Pt(PEt₃)₂Cl₂] (65.8 mg, 0.131 mmol), and CuI (12.5 mg, 0.066 mmol) in CHCl₃/iPr₂NH (v/v 1:1, 15 mL), the product (168 mg, 94%; 88 mg, 49% after precipitation) was obtained as a yellow powder. ¹H NMR (300 MHz, CDCl₃): $\delta=7.12$ –7.35 (m, 14H; ArH), 6.98–7.12 (m, 4H; ArH), 6.90 (s, 4H; core-ArH), 6.23–6.42 (m, 6H; ArH), 3.73–4.02 (m, 12H; ArOCH₂), 2.53–2.94 (m, 12H; ArCH₂+PhCH₂), 2.11–2.43 (m, 12H; PCH₂), 1.88–2.11 (m, 12H; ArCH₂CH₂+PhCH₂CH₂), 1.07–1.37 ppm (m, 18H; PCH₂CH₃); ¹³C NMR (75 MHz, CDCl₃): $\delta=160.3$, 160.1, 153.3, 144.2, 144.0, 141.7, 138.4, 131.0, 128.7, 128.5, 128.3, 126.6, 126.0, 115.5, 109.2 (C≡Cpt), 107.7, 107.3, 107.2, 106.8 (t, ²J(C,P)=14.3 Hz; C≡Cpt), 99.0, 67.7, 66.9, 65.9, 32.6, 32.3, 32.1, 31.5, 31.3, 31.0, 30.9, 16.4 (quintet like, ¹J(C,P)=17.5 Hz; PCH₂), 8.5 ppm; ³¹P NMR (122 MHz, CDCl₃): δ =(major peak): 11.0 (¹J(Pt,P)=2380 Hz); (minor peaks): 14.8 (t, ¹J(Pt,P)=2390 Hz), 10.4 (¹J(Pt,P)=2370 Hz), 8.5 ppm (¹J(Pt,P)=2330 Hz).

Pt-L-G2: Starting from L-G2 (263 mg, 0.131 mmol), *trans*-[Pt(PEt₃)₂Cl₂] (65.8 mg, 0.131 mmol), and CuI (12.5 mg, 0.066 mmol) in CHCl₃/iPr₂NH (v/v 1:1, 15 mL), the product (286 mg, 90%; 227 mg, 71% after precipitation) was obtained as a yellow powder. ¹H NMR (300 MHz, CDCl₃): $\delta=7.11$ –7.37 (m, 34H; ArH), 6.97–7.11 (m, 4H; ArH), 6.81 (s, 4H; core-ArH), 6.21–6.43 (m, 18H; ArH), 3.72–4.05 (m, 28H; ArOCH₂), 2.59–2.93 (m, 28H; ArCH₂+PhCH₂), 2.12–2.33 (m, 12H; PCH₂), 1.94–2.12 (m, 28H; ArCH₂CH₂+PhCH₂CH₂), 1.08–1.34 ppm (m, 18H; PCH₂CH₃); ¹³C NMR (75 MHz, CDCl₃): $\delta=160.2$, 153.2, 144.0, 143.9, 143.8, 141.5, 138.3, 130.9, 128.5, 128.4, 128.2, 126.5, 125.9, 115.4, 109.2 (C≡Cpt), 107.4, 107.1, 106.8 (t, ²J(C,P)=16.3 Hz; C≡Cpt), 99.4, 98.9, 67.7, 67.5, 66.8, 66.0, 32.7, 32.5, 32.2, 32.0, 31.4, 30.9, 30.7, 16.3 (quintet like, ¹J(C,P)=17.5 Hz; PCH₂), 8.4 ppm; ³¹P NMR (122 MHz, CDCl₃): δ =(major peak): 11.1 (¹J(Pt,P)=2380 Hz); (minor peaks): 15.0 (¹J(Pt,P)=2390 Hz), 8.7 ppm (¹J(Pt,P)=2330 Hz).

Pt-L-G3: Starting from L-G3 (194 mg, 0.047 mmol), *trans*-[Pt(PEt₃)₂Cl₂] (23.5 mg, 0.047 mmol), and CuI (4.5 mg, 0.023 mmol) in CHCl₃/iPr₂NH (v/v 1:1, 5.4 mL), the product (204 mg, 95%; 193 mg, 90% after precipitation) was obtained as a yellow powder. ¹H NMR (300 MHz, CDCl₃): $\delta=6.97$ –7.36 (m, 78H; ArH), 6.82 (s, 4H; core-ArH), 6.17–6.46 (m, 42H; ArH), 3.73–4.03 (m, 60H; ArOCH₂), 2.57–2.92 (m, 60H; ArCH₂+PhCH₂), 1.88–2.33 (m, 72H; PCH₂+ArCH₂CH₂+PhCH₂CH₂), 1.06–1.40 ppm (m, 18H; PCH₂CH₃); ¹³C NMR (75 MHz, CDCl₃, the C≡Cpt signal was too weak to be observed): $\delta=160.3$, 160.2, 153.2, 144.0, 143.94, 143.88, 141.6, 138.4, 130.9, 128.6, 128.5, 128.2, 126.0, 115.4, 109.2 (C≡Cpt), 107.2, 99.0, 67.6, 66.93, 66.86, 32.5, 32.2, 32.0, 30.9, 30.8, 30.7, 16.4 (quintet like, ¹J(C,P)=17.7 Hz; PCH₂), 14.8, 14.6, 14.3, 8.45, 8.4, 8.1 ppm; ³¹P NMR (122 MHz, CDCl₃): δ =(major peak): 11.0 (¹J(C,P)=2380 Hz); (minor peaks): 14.9 (¹J(C,P)=2390 Hz), 8.6 ppm (¹J(C,P)=2330 Hz).

Acknowledgement

We thank the Research Grants Council, Hong Kong SAR, for financial support (Project No: 400404).

- [1] For recent examples, see: a) L. M. Passeno, M. E. Mackay, G. L. Baker, R. Vestberg, C. J. Hawker, *Macromolecules* **2006**, *39*, 740–746; b) K. T. Kim, M. A. Winnik, I. Manners, *Soft Matter* **2006**, *2*,

- 957–965; c) B.-K. Cho, A. Jain, S. M. Gruner, U. Wiesner, *Chem. Commun.* **2005**, 2143–2145.
- [2] For recent reviews, see: a) A. Zhang, L. Shu, Z. Bo, A. D. Schlüter, *Macromol. Chem. Phys.* **2003**, *204*, 328–339; b) A. D. Schlüter, *C. R. Chim.* **2003**, *6*, 843–851; c) A. D. Schlüter, *Top. Curr. Chem.* **2005**, *245*, 151–191; d) H. Frauenrath, *Prog. Polym. Sci.* **2005**, *30*, 325–384.
- [3] R. N. Ganesh, J. Shraberg, P. G. Sheridan, S. Thayumanavan, *Tetrahedron Lett.* **2002**, *43*, 7217–7220.
- [4] a) G. R. Newkome, C. N. Moorefield, F. Vögtle, *Dendritic Molecules. Concepts, Syntheses, Perspectives*, Wiley-VCH, Weinheim, **1996**, chap. 9; b) G. R. Newkome, C. N. Moorefield, F. Vögtle, *Dendrimers and Dendrons. Concepts, Syntheses, Applications*, Wiley-VCH, Weinheim, **2001**, chap. 9.
- [5] H.-F. Chow, C.-F. Leung, W. Li, K.-W. Wong, L. Xi, *Angew. Chem.* **2003**, *115*, 5069–5073; *Angew. Chem. Int. Ed.* **2003**, *42*, 4919–4923.
- [6] K. Sonogashira, Y. Tohda, N. Hagihara, *Tetrahedron Lett.* **1975**, *16*, 4467–4470.
- [7] C. Hawker, J. M. J. Fréchet, *J. Am. Chem. Soc.* **1990**, *112*, 7638–7647.
- [8] a) A. S. Hay, *J. Org. Chem.* **1960**, *25*, 1275–1276; b) A. S. Hay, *J. Org. Chem.* **1962**, *27*, 3320–3321.
- [9] A.-D. Schlüter, *Top. Curr. Chem.* **1998**, *197*, 165–191.

Received: November 6, 2008
Published online: January 16, 2009